Tunable Electrical Properties of Silicon Nanowires *via* Surface-Ambient Chemistry

G. D. Yuan,[†] Y. B. Zhou,[†,‡] C. S. Guo,[†] W. J. Zhang,[†,*] Y. B. Tang,[†] Y. Q. Li,[†,§] Z. H. Chen,[†] Z. B. He,[†] X. J. Zhang,[†,§] P. F. Wang,[‡,*] I. Bello,[†] R. Q. Zhang,[†] C. S. Lee,[†] and S. T. Lee[†,*]

[†]Centre of Super-Diamond and Advanced Films (COSDAF) and Department of Physics and Materials Science, City University of Hong Kong, Hong Kong SAR, China, [‡]Key Laboratory of Photochemical Conversion and Optoelectronic Materials, Technical Institute of Physics and Chemistry, Chinese Academy of Sciences, Beijing 100190, China, and [§]Functional Nano & Soft Materials Laboratory (FUNSOM), Soochow University, Suzhou, Jiangsu 215123, China

ABSTRACT p-Type surface conductivity is a uniquely important property of hydrogen-terminated diamond surfaces. In this work, we report similar surface-dominated electrical properties in silicon nanowires (SiNWs). Significantly, we demonstrate tunable and reversible transition of $p^+-p-i-n-n^+$ conductance in nominally intrinsic SiNWs *via* changing surface conditions, in sharp contrast to the only p-type conduction observed on diamond surfaces. On the basis of Si band energies and the electrochemical potentials of the ambient (pH value)-determined adsorbed aqueous layer, we propose an electron-transfer-dominated surface doping model, which can satisfactorily explain both diamond and silicon surface conductivity. The totality of our observations suggests that nanomaterials can be described as a core—shell structure due to their large surface-to-volume ratio. Consequently, controlling the surface or shell in the core—shell model represents a universal way to tune the properties of nanostructures, such as *via* surface-transfer doping, and is crucial for the development of nanostructure-based devices.

KEYWORDS: silicon nanowires · electronic properties · surface charge-transfer doping · core—shell model · field-effect transistors

Semiconductor nanowires are potentially powerful building blocks in integrated nanodevices and systems.[1−11] The ability to rationally synthesize nanowires with precisely controlled and tunable electrical transport properties has opened myriad opportunities for assembling various functional nanosystems, such as photodetectors,[1] multicolor LEDs,[5] 3D integrated electronics,[7] and address decoders.[11] Nanomaterial-based chemo- and biosensors with exceptionally high sensitivity have been demonstrated recently. Surface-sensitive properties of nanostructures form the basis of high-sensitivity gas, chemical and biological detectors. The large surface-to-volume ratio of nanostructures results in the dominance of surface characteristics (*e.g.*, composition, bonding, and surface states/defects) in determining the global (*i.e.*, observed) materials properties (electrical, thermal, mechanical, catalytic, optical, *etc.*) of nanomaterials. However, such high surface sensitivity, though beneficial for some device applications, presents a serious challenge to device fabrication as it leads to difficulty in the reproducibility and controllability of device performances. Nanodevice performance depends sensitively on fabrication procedures, environmental conditions/adsorbates, surface scattering, and surface trapping. Obviously, the ability to control surface properties in nanostructures is fundamental to the development of nanostructure-based devices. In this work, using intrinsic silicon nanowires (SiNWs) as a model system, we demonstrate the role of controlling surface conditions in determining the overall electrical and transport properties of SiNWs.

SiNWs are particularly interesting due to their ready compatibility with present silicon-based semiconductor technology and being a promising candidate for the "bottom-up" approach to nanoscale devices.[2,8−10,12−24] Recent developments have shown diverse applications of SiNWs, such as electronic devices,[2,10,12−15] LEDs,[16] thermoelectric devices,[17] photovoltaics,[18−20] biological or chemical sensors,[21,22] and lithium batteries.[23,24] Doping of semiconductor nanowires is usually achieved by incorporating foreign atoms into the host lattice, *via* post-annealing[25] ion implantation[26] or *in situ* doping during growth *etc.*,[2,12,13,27−29] although each technique has its inherent problems. For example, post-annealing process can lead to reduced near-band-edge (NBE) emission, while ion implantation invariably induces defects and increased resistivity in NWs.[25,26] Further, it is difficult to achieve controlled doping *via* these two methods. By comparison, the

*Address correspondence to apwjzh@cityu.edu.hk (W.J. Zhang), wangpf@mail.ipc.ac.cn (P.F. Wang), apannale@cityu.edu.hk (S.T. Lee).

Received for review January 27, 2010 and accepted May 11, 2010.

Published online May 19, 2010.
10.1021/nn1001613

© 2010 American Chemical Society

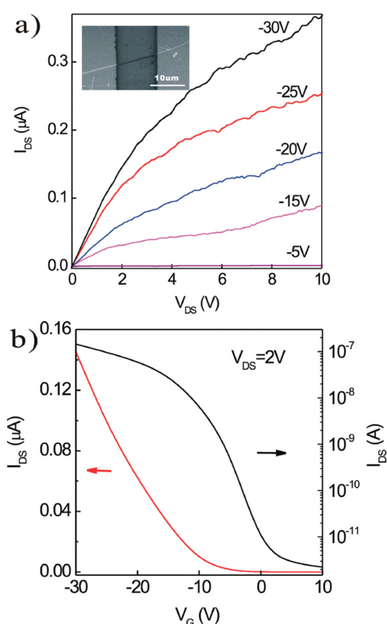

Figure 1. Electrical transport properties of a typical intrinsic SiNW FET (in the inset of a) measured in air with Au (100 nm) as electrodes. Nanowire diameter is 150 nm, and effective gate length is 11 μm. (a) $I_{DS}-V_{DS}$ curves of the device recorded at different V_G. (b) $I_{DS}-V_G$ curves at V_{DS} = 2 V.

in situ doping approach may realize reliable doping profile while keeping the nanostructure intact. Conventionally, dopants are associated with impurity atoms introduced into the bulk of semiconductors. Nevertheless, doping effect can also be achieved *via* electron exchange between the semiconductor and surface adsorbents.[30−38] Indeed, a doping method based on electron transfer, named surface-transfer doping, has been shown for diamond films,[30−34] carbon nanotubes,[35−37] and porous silicon,[38] for which tunable electrical properties have been obtained by chemiadsorption from ambient rather than by dopant introduction into bulk materials. For example, H-terminated diamond in ambient air can gain large surface p-type conductivity, and the electronic conductivity of carbon nanotubes can vary drastically upon exposure to different gases, such as NH_3 or NO_2.[35−37] Nevertheless, similar surface-transfer doping of SiNWs yielding tunable electrical properties has never been reported, to our best knowledge. Here, we report for the first time reversible $p^+-p-i-n-n^+$ transition in intrinsic SiNWs *via* surface-transfer doping.

RESULTS AND DISCUSSION

Figure 1a shows the I_{DS} *versus* V_{DS} curves measured in air of a FET fabricated from a single SiNW, and the inset shows a typical scanning electron microscope (SEM) image of a single NW FET. The diameter of the NW is about 150 nm, and effective gate length is 11 μm. The gate voltage dependence of $I_{DS}-V_{DS}$ curves reveals a pronounced gating effect characteristic of p-type conductivity; that is, the conductance of the NW increases (or decreases) with decreasing (or increasing) positive V_G. The distinctive p-type high conductivity reflects the dominant effect of nanostructures with a large surface-to-volume ratio on transport properties. These results suggest a salient approach (see below) to tune and control doping or conductivity of SiNWs *via* surface adsorption engineering.

The transfer characteristics of the SiNW measured in air at a fixed V_{DS} = 2 V are depicted in Figure 1b. By fitting the linear part of the $I_{DS}-V_G$ curve, transconductance (g_m) value and turn-on threshold voltage (V_{th}) are estimated to be 6 nS and −8.2 V, respectively. The effective field-effect hole mobility (μ_h) can be estimated by using the equation of $g_m = \partial I_{DS}/\partial V_G = \mu_h C V_{DS}/L^2$, where C is the NW capacitance and L is the effective NW length between electrodes. The capacitance is estimated at 1.2×10^{-15} F by the equation of $C = 2\pi\varepsilon_0\varepsilon_{SiO_2}L/\ln(4h/d)$, where ε_{SiO_2} is the dielectric constant of SiO_2, h is SiO_2 thickness, and d is NW diameter. The hole mobility μ_h can then be calculated to be 3.2 $cm^2/(V \cdot s)$ at V_{DS} = 2 V. In addition, the hole concentration (n_h) is estimated to be 3.0×10^{17} cm^{-3} from the equation $n_h = V_{th}C/q\pi(d/2)^2L$, and the resistivity of the SiNW is 1.04 Ωcm according to $\rho = 1/\sigma = 1/nq\mu$, respectively. The resistivity derived here is decreased drastically by about 3 orders of magnitude lower with respect to that of the original wafer surface. Furthermore, the ON/OFF ratio determined from the semilog plot of I_{DS} *versus* V_G at a constant V_{DS} = 2 V is greater than 10^4. Note that the calculated hole mobility is far smaller than that in the original wafer and falls in the low end of the values measured in the p-type or n-type SiNWs synthesized by *in situ* doping method.[2,12,13] The low mobility is understandable because carrier transport in the NW is mainly *via* the thin surface layer rather than the highly insulating core, and the etched NW normally has a rough surface, as shown in Figure S1 (Supporting Information); therefore, scattering centers would severely reduce carrier transport in the NW. We propose that the observed p-type conductivity is due to a surface-transfer doping mechanism,[30−34] by which electrons are transferred from silicon to the outer adsorbate layer, leading to an equal amount of electrons and holes residing on the outer layer and silicon side of the interface, respectively.

It was reported that SiNWs functionalized with 3-aminopropyltriethoxysilane (APTES) and oxide exhibit pH-dependent conductivity, which was explained in terms of change in surface charge *via* protonation and deprotonation.[4] In addition, according to the surface-transfer doping model,[30−34] electrons would transfer from the hydrogen-terminated diamond surface to the adsorbed wet ambient layer when the pH value of the wet layer is less than 7, thereby leading to enhanced p-type conduction in diamond.[32] In light of the similarity of diamond and Si, we propose that p-type conduction in SiNWs is similarly due to the

charge transfer between the SiNW and surrounding ambient environment, which is weakly acidic with pH around 6.

To test our proposed charge-transfer mechanism for p-type conduction and its potential to tune the electrical properties of SiNWs, we performed systematic investigations of the transport characteristics of SiNW FETs in various acidic and basic environments. We measured SiNW FETs in a chamber filled with an acidic ambient and found that the conductance of p-type SiNWs was substantially increased (>4 orders of magnitude) upon exposure to vapors of acetic acid (10%, pH ~5) or nitric acid (10%, pH ~3), as shown in Figure 2a. The experiments were carried out by placing a SiNW FET in a sealed stainless chamber connected to a sealed 500 mL glass flask containing the acid solution. The p-type conductance of the SiNW increased sharply by about 2 orders of magnitude after acetic acid vapor purging for 3 min and then increased slowly by an additional 2 orders of magnitude in 2 h before reaching saturation. In the final saturation stage, we measured the V_G-dependent $I_{DS}-V_{DS}$ curves for the SiNW, as shown in Figure 2b. The wire then exhibited a low resistivity of 8.0×10^{-4} Ωcm and no dependence of $I_{DS}-V_{DS}$ curves on V_G; that is, the curves recorded at V_G of −20, −10, 0, 10, and 20 V were identical and overlapping. The results show that extended exposure to acetic acid vapor led to a high hole concentration in SiNWs, which became nearly metallic-like. Remarkably, after the acetic acid vapor was purged and replaced by pure N_2 at 1000 sccm, the conductance and electrical transport properties of the SiNW recovered within 20 min to almost the original value (Figure 2a).

Similar experiments were conducted by immersing p-type SiNW FETs in the vapor of 10% nitric acid, which has a lower pH value of about 3. The conductance of the exposed p-type SiNW increased to saturation in less than 8 min, much faster than the 2 h needed to reach saturation in acetic acid ambient conditions. After nitric acid vapor was purged and replaced by pure N_2, all transport properties of the SiNW were also completely recovered to those before acid exposure. To ascertain the generality of the phenomenon, we performed extensive experiments and showed that p-type conduction of SiNWs was consistently increased in all acid ambient tested, including acidic gases (CO_2, SO_2, Cl_2, NO_2, and HCl), acid vapors (H_3PO_4, HCl, H_2SO_4, and HF), or weakly acidic organic solutions (alcohol or acetone), whereas p-type conduction of SiNWs was consistently decreased after purging the acid vapor by dry neutral gas of O_2, Ar, or N_2. The decrease in p-type conductivity upon dry gas purging may be attributed to removal of adsorbed water from SiNWs' surface.[30] The totality of the results shows that p-to-p$^+$ transition in the SiNW can be reversibly tuned by adsorption and desorption of acid vapor, and enhanced conductivity and even heavily doped metallic-like p-type conductivity in the

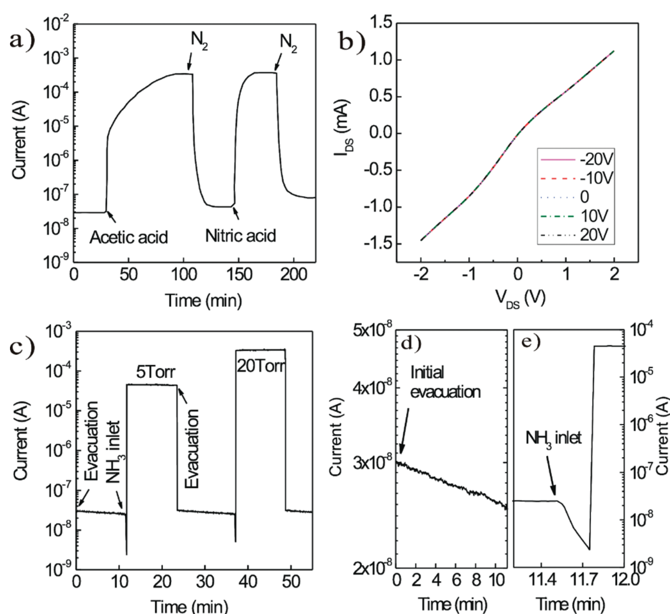

Figure 2. (a) Time dependence of I_{DS} of the SiNW FET measured in air and upon acid purging at V_{DS} = 2 V. (b) $I_{DS}-V_{DS}$ curves at different V_G when the conductance value stabilizes after acetic acid purging. (c) Time dependence of I_{DS} of the SiNW FET measured in vacuum and upon NH_3 purging at V_{DS} = 2 V. (d,e) Expanded views of time dependence of I_{DS} in the initial 12 min in panel c.

SiNW can be realized by exposing the wire to strong or weak acid vapor in the presence of water moisture, with the latter requiring a longer response time.

Next, the response of conductance of SiNW FETs to basic ambient was investigated by introducing 5 sccm of NH_3, a weak base of pH >7, into the chamber; the results are shown in Figure 2c−e. Upon evacuation to vacuum, at a fixed V_{DS} = 2 V, the I_{DS} of the SiNW FET decreased from 3×10^{-8} to 2.5×10^{-8} A in 10 min, as shown in Figure 2d. With NH_3 flowing, Figure 2e shows that the conductance decreased by about 1 order of magnitude in the first ~12 s; the slow change in conductivity sharply contrasts the fast increase in conductance of SiNWs upon exposure to acid vapors. Thereafter, the conductance increased steeply by more than 4 orders of magnitude in 2 s with further inlet of NH_3 before reaching saturation at ~5 Torr. We consider that the dramatic decrease in conductance is due to compensation of the original holes by electrons from the introduced NH_3 at high pH. Consequently, SiNWs changed from p-type to intrinsic, and then to n-type, which corresponds to the subsequent sharp increase in conductance. Once the NH_3 flow was stopped and evacuation started, the conductance and electrical transport properties of the SiNW recovered within 2 s to the original values before the NH_3 purge (Figure 2c). This recovery process exhibited a much faster response than that in acetic or nitric acid vapor. Interestingly, exposure to a second cycle of vacuum and NH_3 vapor at a higher pressure of 20 Torr led to 1 order of magnitude higher equivalent conductance in the SiNW relative to

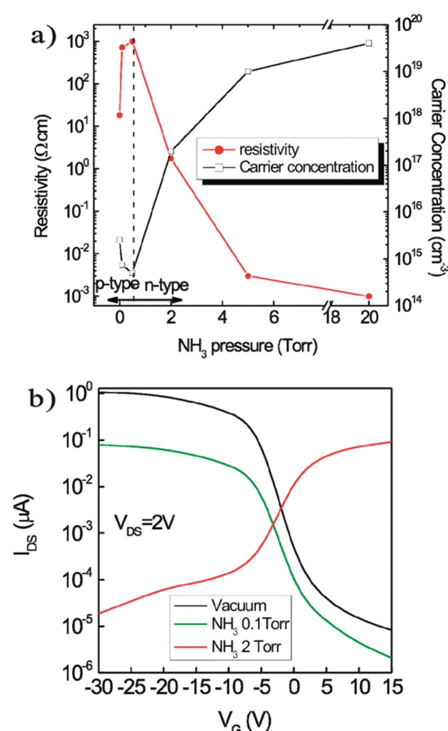

Figure 3. (a) Electrical properties measured under different NH_3 partial pressure. (b) $I_{DS}-V_G$ curves at V_{DS} = 2 V for the SiNW FET in vacuum and at NH_3 pressure of 0.1 and 2 Torr.

that at 5 Torr, as shown in Figure 2c, probably due to more electron injection in NH_3 ambient environment.

The carrier transport properties *versus* NH_3 pressure are shown in Figure 3. From the transfer curves in Figure 3b, SiNWs in vacuum (zero NH_3 pressure) were calculated to have a hole concentration of 2.6×10^{15} cm^{-3} and a resistivity of 18.4 Ωcm, which are 2 and 1 order of magnitude lower and higher than the respective value in air. It suggests that water vapor and CO_2 in ambient air may have a considerable contribution to p-type conduction in SiNWs, thus leading to reduced conductivity upon pumping. At a NH_3 pressure of ~0.1 Torr, the $I_{DS}-V_G$ curves in Figure 3b clearly show ~1 order of magnitude decrease in the conductance of SiNWs relative to that in vacuum; the derived hole concentration and resistivity were 7.4×10^{14} cm^{-3} and 734 Ωcm, respectively. The decreased hole concentration and increased resistivity are attributed to compensation of the free acceptors from the H^+ in acidic air by the free donors from the OH^- in the basic NH_4OH adsorbed layer on SiNW surface. Further increase of NH_3 pressure to 0.5 Torr led to a smaller hole concentration of 5×10^{14} cm^{-3} and a larger resistivity of 1000 Ωcm. We can regard this state of high resistivity as an intrinsic region, which corresponds to the point of minimum carrier concentration in Figure 3a. As the NH_3 pressure increased further to 2 Torr, a transition from highly insulating p-type to lightly resistive n-type is clearly observed in Figure 3b. This result can be explained as due to a charge compensation phenomenon, as shown in Figure 2, in which the electrons injected by NH_3 first

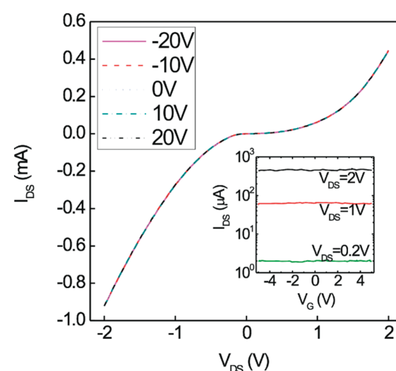

Figure 4. $I_{DS}-V_{DS}$ curves at different V_G of the SiNW FET at NH_3 pressure of 20 Torr.

consume the existing holes in the SiNW surface and then become the majority carrier at high NH_3 pressure, leading to the observed resistivity change in Figure 3. From the $I_{DS}-V_G$ data recorded at this conduction-type changing stage, the electron concentration and resistivity of the n-type SiNWs were deduced to be 2×10^{17} cm^{-3} and 1.76 Ωcm, respectively. In addition, high n-type conductivity in SiNWs was observed (Figure 3a) as the pressure increased further to 5 and 20 Torr, for which the obtained resistivity values were, respectively, 0.003 and 0.001 Ωcm. The $I_{DS}-V_{DS}$ and $I_{DS}-V_G$ curves obtained at 20 Torr of NH_3 are shown in Figure 4, revealing that the $I_{DS}-V_{DS}$ curves of the heavily doped n-type SiNWs are highly nonlinear, but reproducible and independent of V_G. The low resistivity (3 orders of magnitude smaller than that in lightly doped n-type SiNW samples) and V_G independence demonstrate that high electron concentration can also be created in SiNWs *via* exposure to NH_3 at high pressure.

The formation of Schottky contacts between metal electrodes and SiNWs leads to the nonlinear $I_{DS}-V_{DS}$ curves, and it is known that the Schottky barrier may influence strongly the FET characteristics. In this work, besides Au electrodes, we also fabricated and characterized SiNW-based FETs using source and drain electrodes of different work functions, such as Ti/Au (90/10 nm) and Ni/Au (90/10 nm). Nevertheless, for a specific electrode material, although the $I_{DS}-V_{DS}$ curves may show poor linearity, the FETs demonstrate clearly different responses with p- and n-type channels to acidic and basic environments, respectively. The results show that it is the response of SiNW channels to ambient conditions rather than the variations of work functions of electrodes or Schottky barrier heights that determines the corresponding conductance variation and final FET characteristics in different ambient environments.

We next investigated the mechanisms of the p-type dominant transport nature of low resistivity in SiNWs that are etched from a high-insulating Si wafer. A series of systematic experiments showed that p-type conductivity was consistently observed in SiNWs etched from intrinsic, p-type, or even n-type wafer irrespective of surface orientation, as long as the SiNWs were

H-terminated.[39] However, p-type conductivity would disappear and return to the original high resistivity of the mother Si wafer if SiNWs were dehydrogenated or oxidized to O-termination prior to device fabrication. We found that the non-intentionally doped SiNWs grown by oxide-assisted growth *via* thermal evaporation of SiO powder[8] and terminated with hydrogen also exhibited p-type conductivity. Thus, the hole-dominant conductivity is present in all H-terminated SiNWs irrespective of their synthetic scheme. This is similar to the p-type surface conductivity in diamond films,[30−34] and *ab initio* calculations also indicate that H-termination solely is a necessary condition for the p-type conduction in SiNWs.[40]

In this work, the SiNWs are synthesized by etching in diluted HF solutions. Miyazaki *et al.* have observed a Fermi level position near midgap at the surface of hydrogen-passivated Si surfaces independent of p-type or n-type doping.[41] On the basis of the annealing behavior of E_F points, they suggested a near surface depletion layer caused by hydrogen passivation of dopants during the wet chemical surface treatment as the likely cause. However, we believe the formation of such a surface depletion layer by hydrogen passivation plays a less important role in our observations. First, the etched intrinsic SiNWs show either p- or n-type conduction determined by the ambient chemistry, and second, if a surface depletion layer is induced independent of doping, the conductivity of p-type SiNWs (etched from p-type wafers) should decrease in the ambient air, which is in contrast to our observations of an increased conductivity in ref 39. Furthermore, our repeated experiments also revealed that vacuum annealing at 150−250 °C for 30 min can convert the p-type conduction of SiNWs to its original highly insulating state. Full reversibility of conductivity upon a complete cycle of vacuum annealing and air exposure of SiNWs can be preserved as long as the annealing temperature is limited to the range of 150−250 °C. A reasonable explanation for the reversible removal of the p-type conduction in SiNWs is that the moisture layer is removed but hydrogen termination of SiNWs remains intact upon moderate vacuum thermal annealing.[42] We suppose that the wet layer due to the moisture water in air at the SiNW surface provides an electrolyte, in which the electron exchange between the SiNW and ambient occurs, thereby leading to the conductive surface in insulating SiNWs. Furthermore, the p-type conduction rather than n-type is due to the weak acidic properties of air, which yields a pH value of ~6 due to CO_2.

In the following, we use band diagrams of Si surfaces to explain the dependence of electrical transport properties of SiNWs on the surrounding ambient environment. The energy levels of Si are given in Figure 5 with respect to the vacuum reference, together with those of H-terminated diamond for comparison. The electron affinity (EA) of clean Si in vacuum is around 4.05 eV[42] and down-shifted to 4.17 eV after hydrogenation.[43] Since the band gap of Si is 1.12 eV,[42] the position of the conduction band minimum (E_C), the Fermi level (E_F), and the valence band maximum (E_V) of hydrogenated SiNWs are placed at −4.17, −4.73 (in the middle of the gap), and −5.29 eV, respectively.

A surface charge-transfer model *via* redox reactions in the absorbed water surface-cover layer was proposed by Maier *et al.*[30] for the surface conduction of diamond, which was then augmented by the oxygen redox couple proposed by Foord *et al.*[31] and Chakrapani *et al.*[32] However, the models proposed for diamond thus far cannot be applied directly to experimental observations of SiNWs reported here. For example, Chakrapani *et al.*[32] suggested that the electrochemical potential or Fermi level (μ_e) of the surface wet layer in ambient air can be determined by an oxygen redox couple reaction $O_2 + 4H^+ + 4e^- \rightleftharpoons 2H_2O$, and the μ_e values are given by Nernst equation and the maximum practical energy range of the oxygen redox couple varies from −5.66 eV at pH = 0 to −4.83 eV at pH = 14, as shown in Figure 5a. Therefore, E_F (−4.73 eV) in Si is higher than the largest μ_e (−4.83 eV for pH = 14) in the proposed model of Chakrapani *et al.*[32] As a result, electrons could only transfer from Si to the wet layer, leading to the electrochemical pinning of the Fermi level and only p-type transport properties in SiNWs, as shown in Figure 5b. It is clear that the proposed oxygen redox couple reaction is not consistent with our experimental results, which showed that both p and n conduction in SiNWs is possible upon changing the pH values of the ambient environment. Maier *et al.*[30] suggested another model, in which μ_e is determined by the hydrogen redox reaction $2H_3O + 2e^- \rightleftharpoons H_2 + 2H_2O$. According to this model, μ_e is in the range from −4.61 eV at pH = 0 to −3.80 eV at pH = 14, as shown in Figure 5a. However, μ_e is −4.27 eV at pH = 6 for air, which is higher than the Fermi level in SiNWs. Accordingly, electrons would flow from the surrounding ambient into SiNWs, and n-type conduction of SiNWs would be induced, which also is at variance with our experimental observations.

As shown in Figure 5, both of the above models can explain the p-type only surface conductivity in hydrogen-terminated diamond but cannot explain our experimental conductivity results of SiNWs. We therefore propose a model that considers the redox reactions involving both H_2 and O_2. Since O_2 and H_2 coexist in air, we propose that the μ_e value in ambient air is associated with both the oxygen and the hydrogen redox couples, and the μ_e value at pH = 7 is determined by the partial pressures of H_2 and O_2 in the aqueous layer. On the basis of the experimental results, we suppose that the μ_e value should be aligned to the Fermi energy of SiNWs (−4.73 eV) at pH = 7, as shown in Figure 5a. Consequently, electrons would transfer from SiNWs to the adsorbed layer at pH < 7 and *vice versa* at pH > 7. It then follows that exposure of SiNWs to

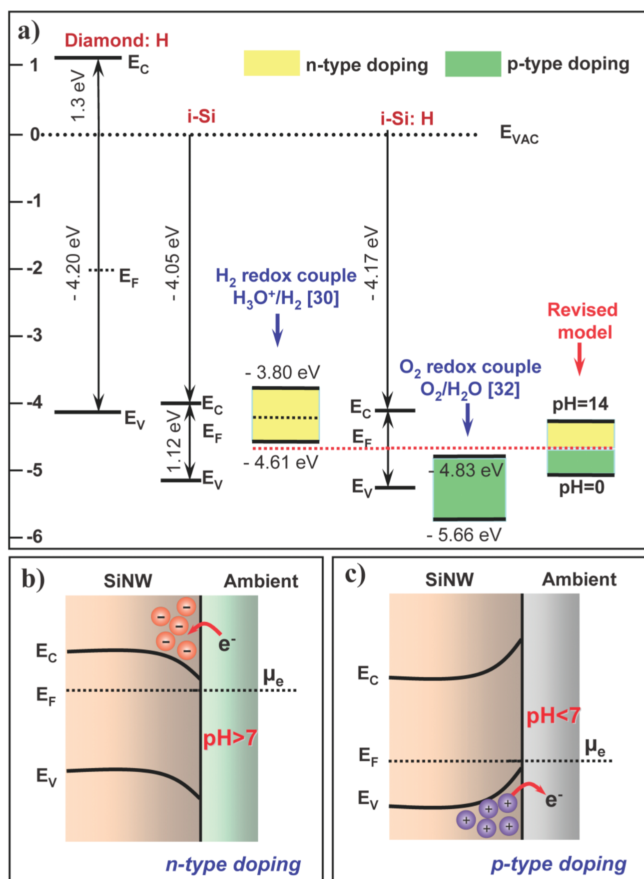

Figure 5. (a) Schematic energy levels of hydrogenated SiNW surface in contact with a wet layer in ambient air. (b,c) Band bending under n- and p-type doping *via* electron-transfer process at the interface between the SiNW and the wet layer.

acidic ambient conditions with pH < 7 would lead to an enhancement of p-type conduction, while exposure to a basic ambient with pH > 7 would convert SiNWs to n-type conduction, as shown in Figure 5b,c. Note that our modified model can also account for the p-type surface conductivity of hydrogen-terminated diamond. Moreover, the current mechanism can similarly explain the dramatic increase in electron carrier concentration in n-type porous Si upon adsorption of ammonia,[38] for which no explanation has been given.

We advocate that the surface-transfer doping should have a universal effect on the surface conductivity of most materials in an appropriate surrounding ambient, although it may become noticeable only in bulk materials that are highly insulating relative to the surface conducting layer. Fox example, surface conductivity in hydrogen-terminated diamond readily reveals the surface-transfer doping effect because the surface conductivity of diamond at room temperature is typically at $10^{-5}-10^{-4}\ \Omega^{-1}\ cm^{-1}$, which is some 13 orders higher than the bulk conductivity of undoped diamond at $10^{-18}-10^{-17}\ \Omega^{-1}\ cm^{-1}$.[30] Recent transport measurements showed that the electronic conductivity in Si in thin silicon-on-insulator (SOI) is primarily determined not by the bulk dopants but by the interaction of surface or interface electronic energy levels with the band structure of the thin silicon template layer.[44] The "exceptional" conductivity in the nanoscale Si membranes in SOI becomes noticeable because its value of $10^{-6}-10^{-5}\ \Omega^{-1}\ cm^{-1}$ is some 10 orders of magnitude larger than that of the substrate SiO_2 at $10^{-16}-10^{-14}\ \Omega^{-1}\ cm^{-1}$. It also explains why surface conductivity cannot be observed in Si wafer because bulk Si conductivity is comparably high at $10^{-6}-10^{-5}\ \Omega^{-1}\ cm^{-1}$. It has been suggested that the surface-transfer doping effect would extend to a layer of 30 nm below the surface of diamond.[30] In light of the affected surface layer, we suppose that any given bulk films or nanomaterials can be described as a core−shell (or bulk-surface) composite structure. Such a model arises from the fact that for the nanosized materials a large fraction of the atoms/molecules resides on the surface or shell region where they are exposed to a distinctly and fundamentally different environment from the core. Therefore, the performance of any nanodevices would depend critically on the fabrication procedures, environmental conditions/adsorbates, surface scattering, and surface trapping.

Clearly, the ability to control the surface properties in nanostructures is crucial for the development of nanostructure-based devices, in particular, in those which involve a chemical environment (liquid or gas) around the nanowires such as nanosensors for biological or chemical species, lithium ion batteries, dye-sensitized solar cells, and photoelectrochemical cells. The surface-transfer doping effect affects not only the electrical properties but also other materials properties, in general, including electronic, optical, photonic, thermal, thermoelectric, mechanical, catalytic, chemical, biological, and biomedical sensing, *etc*. Since hydrogen termination plays an essential role in surface-transfer doping of SiNWs, the stability of Si−H bonding on SiNW surfaces is an important consideration for practical applications. Previous experiments on annealing of high-surface-area porous silicon samples in an ultrahigh vacuum revealed that hydrogen from SiH and SiH_2 species on H-terminated silicon surfaces formed by HF treatment desorbed between 720−800 and 640−700 K, respectively,[45] suggesting reasonable thermal stability of Si−H bonding. Nevertheless, it has also been noted that H-terminated silicon surfaces were oxidized gradually on exposure to air, especially in the presence of water.[46] Although H-terminated surfaces of small-diameter SiNWs were shown to be chemically more inert against oxidation than H-terminated silicon wafer surface,[8] chemical stability of H-terminated SiNWs remains a concern to be addressed.

CONCLUSION

In summary, we demonstrate a unique controllable doping method, which can tune the electrical and transport properties of SiNWs *via* simple chemi-

adsorption, namely, surface-transfer doping.[30−34] SiNWs prepared by etching an intrinsic Si wafer exhibit distinctly p-type transport properties in ambient air, which are attributed to the weak acidic properties of normal air. The light p-type conductivity of SiNWs in air could be changed to metallic-like p-type *via* exposure to acid vapor, such as weak acetic acid or strong nitric acid. Further, the light p-type conduction of SiNWs could be changed to intrinsic or high resistivity upon exposure to NH_3 and to lightly n-type and eventually metallic-like n-type conductivity with increasing NH_3 pressure. We propose that the pH values around SiNWs are more critical in determining the electrical properties of SiNWs than hydrogenation and water vapor in air *via* surface-transfer doping. The surface charge transfer is expected to have a general effect on nanostructures and on the performance and applications of devices based on nanostructures.

EXPERIMENTAL SECTION

SiNWs were synthesized by etching intrinsic a Si(111) wafer using our metal-assisted etching method[9,24] (see also Supporting Information) and had diameters of 50−250 nm with an average of 150 nm. The intrinsic Si wafer had a resistivity of 1.4×10^4 Ωcm, a bulk hole concentration of 9.3×10^{11} cm^{-3}, and a mobility of 470 $cm^2/(V \cdot s)$. For the fabrication of single SiNW field-effect transistors (FETs), SiNWs were collected from the etched wafer and dispersed in alcohol. The resulting SiNW suspension was spread on a SiO_2 (300 nm)/p^+-Si wafer at a desired density. Deposition of 100 nm Au *via* a shadow mask was performed to pattern the electrodes on individual SiNWs. The gate voltage was applied to the p^+-Si substrate in standard global back-gate geometry.

Acknowledgment. The work was supported by the Research Grants Council of Hong Kong SAR, China CRF Grant (No. CityU5/CRF/08) and RGC/NSFC Joint Research Grant (No. N_CityU 108/08), the National Basic Research Program of China (973 Program) (Grant Nos. 2006CB933000 and 2007CB936000).

Supporting Information Available: Materials and methods. This material is available free of charge *via* the Internet at http://pubs.acs.org.

REFERENCES AND NOTES

1. Yang, C.; Barrelet, C. J.; Capasso, F.; Lieber, C. M. Single p-Type/Intrinsic/n-Type Silicon Nanowires as Nanoscale Avalanche Photodetectors. *Nano Lett.* **2006**, *6*, 2929–2934.
2. Cui, Y.; Duan, X. F.; Hu, J. T.; Lieber, C. M. Doping and Electrical Transport in Silicon Nanowires. *J. Phys. Chem. B* **2000**, *104*, 5213–5216.
3. Cui, Y.; Lieber, C. M. Functional Nanoscale Electronic Devices Assembled Using Silicon Nanowire Building Blocks. *Science* **2001**, *291*, 851–853.
4. Cui, Y.; Wei, Q. Q.; Park, H. K.; Lieber, C. M. Nanowire Nanosensors for Highly Sensitive and Selective Detection of Biological and Chemical Species. *Science* **2001**, *293*, 1289–1292.
5. Duan, X. F.; Huang, Y.; Cui, Y.; Wang, J. F.; Lieber, C. M. Indium Phosphide Nanowires as Building Blocks for Nanoscale Electronic and Optoelectronic Devices. *Nature* **2001**, *409*, 66–69.
6. Huang, Y.; Duan, X. F.; Cui, Y.; Lauhon, L. J.; Kim, K. H.; Lieber, C. M. Logic Gates and Computation from Assembled Nanowire Building Blocks. *Science* **2001**, *294*, 1313–1317.
7. Javey, A.; Nam, S.; Friedman, R. S.; Yan, H.; Lieber, C. M. Layer-by-Layer Assembly of Nanowires for Three-Dimensional, Multifunctional Electronics. *Nano Lett.* **2007**, *7*, 773–777.
8. Ma, D. D. D.; Lee, C. S.; Au, F. C. K.; Tong, S. Y.; Lee, S. T. Small-Diameter Silicon Nanowire Surfaces. *Science* **2003**, *299*, 1874–1877.
9. Peng, K. Q.; Hu, J. J.; Yan, Y. J.; Wu, Y.; Fang, H.; Xu, Y.; Lee, S. T.; Zhu, J. Fabrication of Single-Crystalline Silicon Nanowires by Scratching a Silicon Surface with Catalytic Metal Particles. *Adv. Funct. Mater.* **2006**, *16*, 387–394.
10. Park, W. I.; Zheng, G.; Jiang, X.; Tian, B.; LIeber, C. M. Controlled Synthesis of Millimeter-Long Silicon Nanowires with Uniform Electronic Properties. *Nano Lett.* **2008**, *8*, 3004–3009.
11. Zhong, Z. H.; Wang, D. L.; Cui, Y.; Bockrath, M. W.; Lieber, C. M. Nanowire Crossbar Arrays as Address Decoders for Integrated Nanosystems. *Science* **2003**, *302*, 1377–1379.
12. Cui, Y.; Zhong, Z. H.; Wang, D. L.; Wang, W. U.; Lieber, C. M. High Performance Silicon Nanowire Field Effect Transistors. *Nano Lett.* **2003**, *3*, 149–152.
13. Zheng, G.; Lu, W.; Jin, S.; Lieber, C. M. Synthesis and Fabrication of High-Performance n-Type Silicon Nanowire Transistors. *Adv. Mater.* **2004**, *16*, 1890–1893.
14. Dong, Y; Yu, G; Mcalpine, M. C. L., W; Lieber, C. M. Si/a-Si Core/Shell Nanowires as Nonvolatile Crossbar Switches. *Nano Lett.* **2008**, *8*, 386–391.
15. Hu, Y.; Xiang, J.; Liang, G.; Yan, H.; Lieber, C. M. Sub-100 Nanometer Channel Length Ge/Si Nanowire Transistors with Potential for 2 THz Switching Speed. *Nano Lett.* **2008**, *8*, 925–930.
16. Ng, W. L.; Lourenco, M. A.; Gwilliam, R. M.; Ledain, S.; Shao, G.; Homewood, K. P. An Efficient Room-Temperature Silicon-Based Light-Emitting Diode. *Nature* **2001**, *410*, 192–194.
17. Hochbaum, A. I.; Chen, R. K.; Delgado, R. D.; Liang, W. J.; Garnett, E. C.; Najarian, M.; Majumdar, A.; Yang, P. D. Enhanced Thermoelectric Performance of Rough Silicon Nanowires. *Nature* **2008**, *451*, 163–168.
18. Garnett, E. C.; Yang, P. Silicon Nanowire Radial p−n Junction Solar Cells. *J. Am. Chem. Soc.* **2008**, *130*, 9224–9225.
19. Kempa, T. J.; Tian, B.; Kim, D. R.; Hu, J.; Zheng, X.; Lieber, C. M. Single and Tandem Axial p−i−n Nanowire Photovoltaic Devices. *Nano Lett.* **2008**, *8*, 3456–3460.
20. Tian, B. Z.; Zheng, X. L.; Kempa, T. J.; Fang, Y.; Yu, N. F.; Yu, G. H.; Huang, J. L.; Lieber, C. M. Coaxial Silicon Nanowires as Solar Cells and Nanoelectronic Power Sources. *Nature* **2007**, *449*, 885-8.
21. Zheng, G.; Patolsky, F.; Cui, Y.; Wang, W. U.; Lieber, C. M. Multiplexed Electrical Detection of Cancer Markers with Nanowire Sensor Arrays. *Nat. Biotechnol.* **2005**, *23*, 1294–1301.
22. Hu, Y. J.; Churchill, H. O. H.; Reilly, D. J.; Xiang, J.; Lieber, C. M.; Marcus, C. M. A Ge/Si Heterostructure Nanowire-Based Double Quantum Dot with Integrated Charge Sensor. *Nat. Nanotechnol.* **2007**, *2*, 622–625.
23. Chan, C. K.; Zhang, X. F.; Cui, Y. High Capacity Li-Ion Battery Anodes Using Ge Nanowires. *Nano Lett.* **2007**, *8*, 307–309.
24. Peng, K.; Jie, J.; Zhang, W. J.; Lee, S.-T. Silicon Nanowires for Rechargeable Lithium-Ion Battery Anodes. *Appl. Phys. Lett.* **2008**, *93*, 033105.
25. Li, Y. Q.; Zapien, J. A.; Shan, Y. Y.; Liu, Y. K.; Lee, S. T. Manganese Doping and Optical Properties of ZnS Nanoribbons by Postannealing. *Appl. Phys. Lett.* **2006**, *88*, 013115.
26. Hsin, C. L.; He, J. H.; Lee, C. Y.; Wu, W. W.; Yeh, P. H.; Chen, L. J.; Wang, Z. L. Lateral Self-Aligned p-Type In_2O_3 Nanowire Arrays Epitaxially Grown on Si Substrates. *Nano Lett.* **2007**, *7*, 1799–1803.
27. Yuan, G. D.; Zhang, W. J.; Jie, J. S.; Fan, X.; Tang, J. X.;

ARTICLE

Shafiq, I.; Ye, Z. Z.; Lee, C. S.; Lee, S. T. Tunable n-Type Conductivity and Transport Properties of Ga-Doped ZnO Nanowire Arrays. *Adv. Mater.* **2008**, *20*, 168–173.

28. Yuan, G. D.; Zhang, W. J.; Jie, J. S.; Fan, X.; Zapien, J. A.; Leung, Y. H.; Luo, L. B.; Wang, P. F.; Lee, C. S.; Lee, S. T. p-Type ZnO Nanowire Arrays. *Nano Lett.* **2008**, *8*, 2591–2597.
29. Yuan, G. D.; Zhang, W. J.; Zhang, W. F.; Fan, X.; Bello, I.; Lee, C. S.; Lee, S. T. p-Type Conduction in Nitrogen-Doped ZnS Nanoribbons. *Appl. Phys. Lett.* **2008**, *93*, 213102.
30. Maier, F.; Riedel, M.; Mantel, B.; Ristein, J.; Ley, L. Origin of Surface Conductivity in Diamond. *Phys. Rev. Lett.* **2000**, *85*, 3472–3475.
31. Foord, J. S.; Hian, L. C.; Jackman, R. B. An Investigation of the Surface Reactivity of Diamond Photocathodes with Molecular and Atomic Oxygen Species. *Diamond Relat. Mater.* **2001**, *10*, 710–714.
32. Chakrapani, V.; Angus, J. C.; Anderson, A. B.; Wolter, S. D.; Stoner, B. R.; Sumanasekera, G. U. Charge Transfer Equilibria between Diamond and an Aqueous Oxygen Electrochemical Redox Couple. *Science* **2007**, *318*, 1424–1430.
33. Ristein, J. Surface Transfer Doping of Semiconductors. *Science* **2006**, *313*, 1057–1058.
34. Strobel, P.; Riedel, M.; Ristein, J.; Ley, L. Surface Transfer Doping of Diamond. *Nature* **2004**, *430*, 439–441.
35. Chang, H.; Lee, J. D.; Lee, S. M.; Lee, Y. H. Adsorption of NH_3 and NO_2 Molecules on Carbon Nanotubes. *Appl. Phys. Lett.* **2001**, *79*, 3863–3865.
36. Collins, P. G.; Bradley, K.; Ishigami, M.; Zettl, A. Extreme Oxygen Sensitivity of Electronic Properties of Carbon Nanotubes. *Science* **2000**, *287*, 1801–1804.
37. Kong, J.; Franklin, N. R.; Zhou, C. W.; Chapline, M. G.; Peng, S.; Cho, K. J.; Dai, H. J. Nanotube Molecular Wires As Chemical Sensors. *Science* **2000**, *287*, 622–625.
38. Chiesa, M.; Amato, G.; Boarino, L.; Garrone, E.; Geobaldo, F.; Giamello, E. Reversible Insulator-to-Metal Transition in $p^{(+)}$ -Type Mesoporous Silicon Induced by the Adsorption of Ammonia. *Angew. Chem., Int. Ed.* **2003**, *42*, 5032–5035.
39. Jie, J. S.; Zhang, W. J.; Peng, K. Q.; Yuan, G. D.; Lee, C. S.; Lee, S. T. Surface-Dominated Transport Properties of Silicon Nanowires. *Adv. Funct. Mater.* **2008**, *18*, 3251–3257.
40. Guo, C. S.; Luo, L. B.; Yuan, G. D.; Yang, X. B.; Zhang, R. Q.; Zhang, W. J.; Lee, S. T. Surface Passivation and Transfer Doping of Silicon Nanowires. *Angew. Chem., Int. Ed.* **2009**, *48*, 9896–9900.
41. Miyazaki, S.; Schafer, J.; Ristein, J.; Ley, L. Surface Fermi Level Position of Hydrogen Passivated Si(111) Surfaces. *Appl. Phys. Lett.* **1996**, *68*, 1247–1249.
42. Sze, S. M. *Physics of Semiconductor Devices*; Wiley: New York, 1981.
43. Hunger, R.; Pettenkofer, C.; Scheer, R. Dipole Formation and Band Alignment at the Si(111)/$CuInS_2$ Heterojunction. *J. Appl. Phys.* **2002**, *91*, 6560–6570.
44. Zhang, P. P.; Tevaarwerk, E.; Park, B. N.; Savage, D. E.; Celler, G. K.; Knezevic, I.; Evans, P. G.; Eriksson, M. A.; Lagally, M. G. Electronic Transport in Nanometre-Scale Silicon-on-Insulator Membranes. *Nature* **2006**, *439*, 703–706.
45. Gupta, P.; Colvin, V. L.; George, S. M. Hydrogen Desorption-Kinetics from Monohydride and Dihydride Species on Silicon Surfaces. *Phys. Rev. B* **1988**, *37*, 8234–8243.
46. Niwano, M.; Kageyama, J.; Kurita, K.; Kinashi, K.; Takahashi, I.; Miyamoto, N. Infrared Spectroscopy Study of Initial Stages of Oxidation of Hydrogen-Terminated Si Surfaces Stored in Air. *J. Appl. Phys.* **1994**, *76*, 2157–2163.